5. Supplementary Information.

5.1. (Atom-projected) vibrational spectra

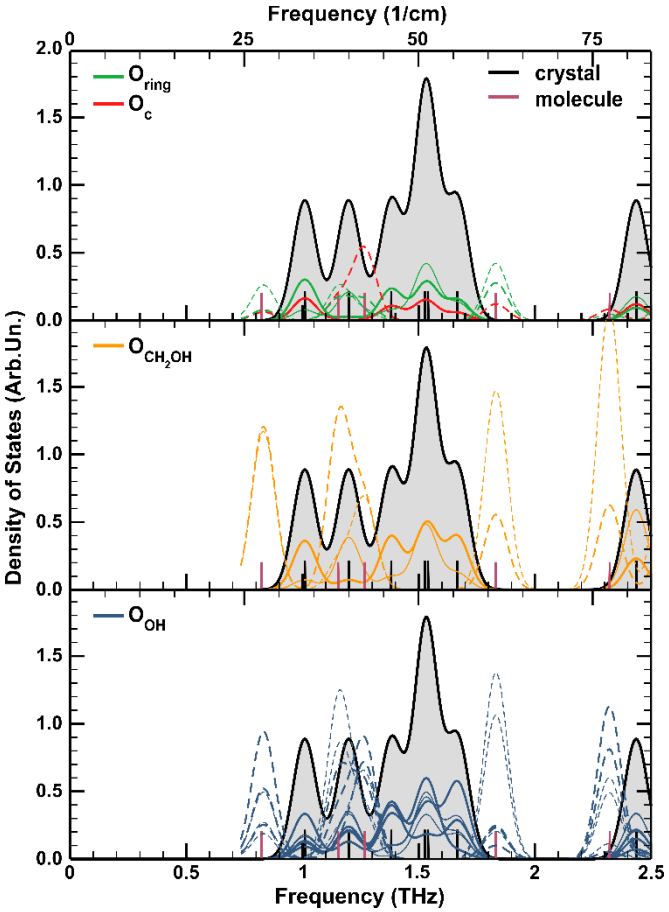

Fig. S1: Atom-projected vibrational DOS of the different O atoms, as defined in Fig. 5a, in the gas-phase and molecular crystal (hygroscopic). Solid lines for the molecular crystal, dashed lines for the gas-phase molecule. The total DOS of the molecular crystal is scaled by a factor 2/9 per molecule to have a range comparable to that of the atom-projected DOS's. The exact position of the Γ-point states of the molecular crystal and gas-phase molecule are indicated by the vertical black and burgundy lines respectively.

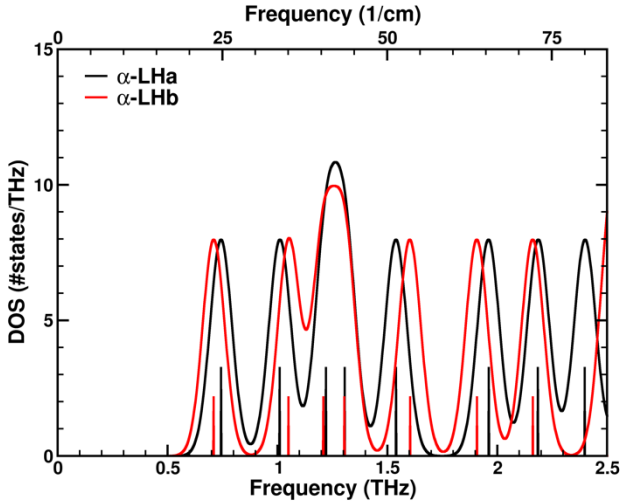

Fig. S2: Low THz vibrational spectrum of the α-LHa (black) and α-LHb (red) configurations. A Gaussian smearing of 0.05THz was employed. The vertical lines indicate the exact position of the Γ-point vibrational modes. Slightly longer lines are used for α-LHa to prevent overlapping modes to be hidden.

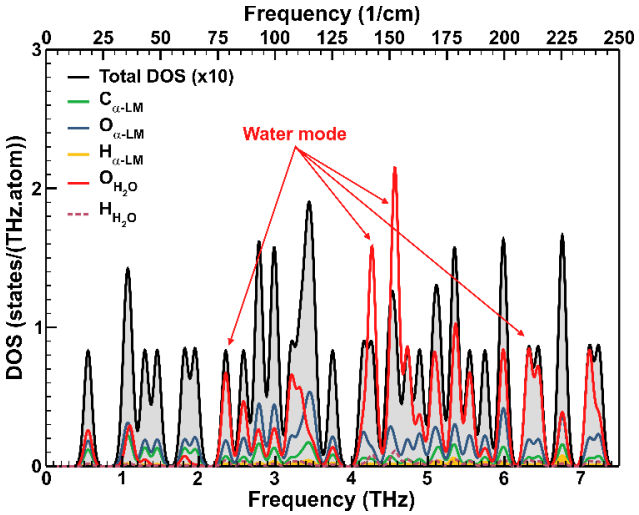

Fig. S3: Atom-projected vibrational spectrum at the Γ-point for the α-LM configuration. The total DOS of the system is scaled by a factor 10 to improve comparison. Note that the α-LM configuration contains two lactose molecules, accounting for 24, 22, and 44 atoms of C, O, and H, respectively. For the atoms belonging to the Lactose molecules the spectrum is averaged per atom. For the atoms of the two water molecules a similar averaging is performed.

5.2. Structure parameters of the simulated systems

Table S1: Structural parameters of the modelled systems. A unit cell contains two Lactose molecules.

System	Volume	a	b	c	α	β	γ	E_0	E_f	E_b	#water
	Å^3	Å	Å	Å	°	°	°	eV	eV	meV/ water	
α-LA	707.42	7.640	19.795	4.915	92.15	106.14	96.59	-533.717	-2.881	NA	0
α-LH	722.69	7.751	19.687	4.883	90	104.09	90	-533.444	-2.745	NA	0
α-LHa	747.15	7.814	20.886	4.823	84.18	106.61	96.77	-548.554	-3.153	-816	1
α-LHb	746.20	7.922	20.934	4.812	96.90	108.90	92.77	-548.577	-3.164	-839	1
α-LM	761.72	7.767	21.541	4.745	90	106.35	90	-563.790	-3.624	-879	2
β-L	707.95	10.845	13.219	4.944	90	92.63	90	-533.532	-2.826	NA	0
αβ-L	712.15	7.441	19.488	5.122	87.05	74.56	84.23	-533.434	-2.758	NA	0

Table S2: Structural parameters of the different (optimized) model systems used to calculate the low THz spectrum of Fig. 9a. The relative total energy with regard to the energy minimum, E_{rel}, is given per unit cell. A unit cell of α-LM contains two Lactose molecules as well as two water molecules.

System	Volume	a	b	c	α	β	γ	E_{rel}
	Å^3	Å	Å	Å	°	°	°	meV/unit cell
α-LM	743.64	7.721	21.398	4.681	90	105.91	90	27
α-LM	761.72	7.767	21.541	4.745	90	106.35	90	0
α-LM	763.00	7.770	21.548	4.750	90	106.37	90	0
α-LM	768.00	7.782	21.589	4.767	90	106.47	90	3
α-LM	768.84	7.807	21.637	4.733	90	105.91	90	390
exp. α-LM[90]	768.84	7.760	21.540	4.783	90	105.91	90	NA

Table S3: Structural parameters of the different optimized model systems used to calculate the low THz spectrum of Fig. 9b. No corrections are performed for Pulay stresses. The reference system with the water molecules fully optimized is indicated as A. The Tait-Bryan angles of the rotated water molecule are given by α_w, β_w, and γ_w.

System	α_w	β_w	γ_w	Volume (opt)	a	b	c	α	β	γ	E_{rel} (not opt)	E_{rel} (opt)
	°	°	°	Å^3	Å	Å	Å	°	°	°	meV / unit cell	meV / unit cell
A	-	-	-	743.64	7.721	21.398	4.681	90	105.91	90	-	0
B	180	140	140	745.11	7.702	21.414	4.695	90.57	105.80	89.98	44	28
B’	160	140	160	745.27	7.706	21.397	4.694	90.56	105.63	89.93	33	16
C	20	180	160	748.62	7.770	21.482	4.663	88.08	105.78	89.94	3765	453

5.3. Ball-and-stick representation of the molecular crystal structures studied in the work

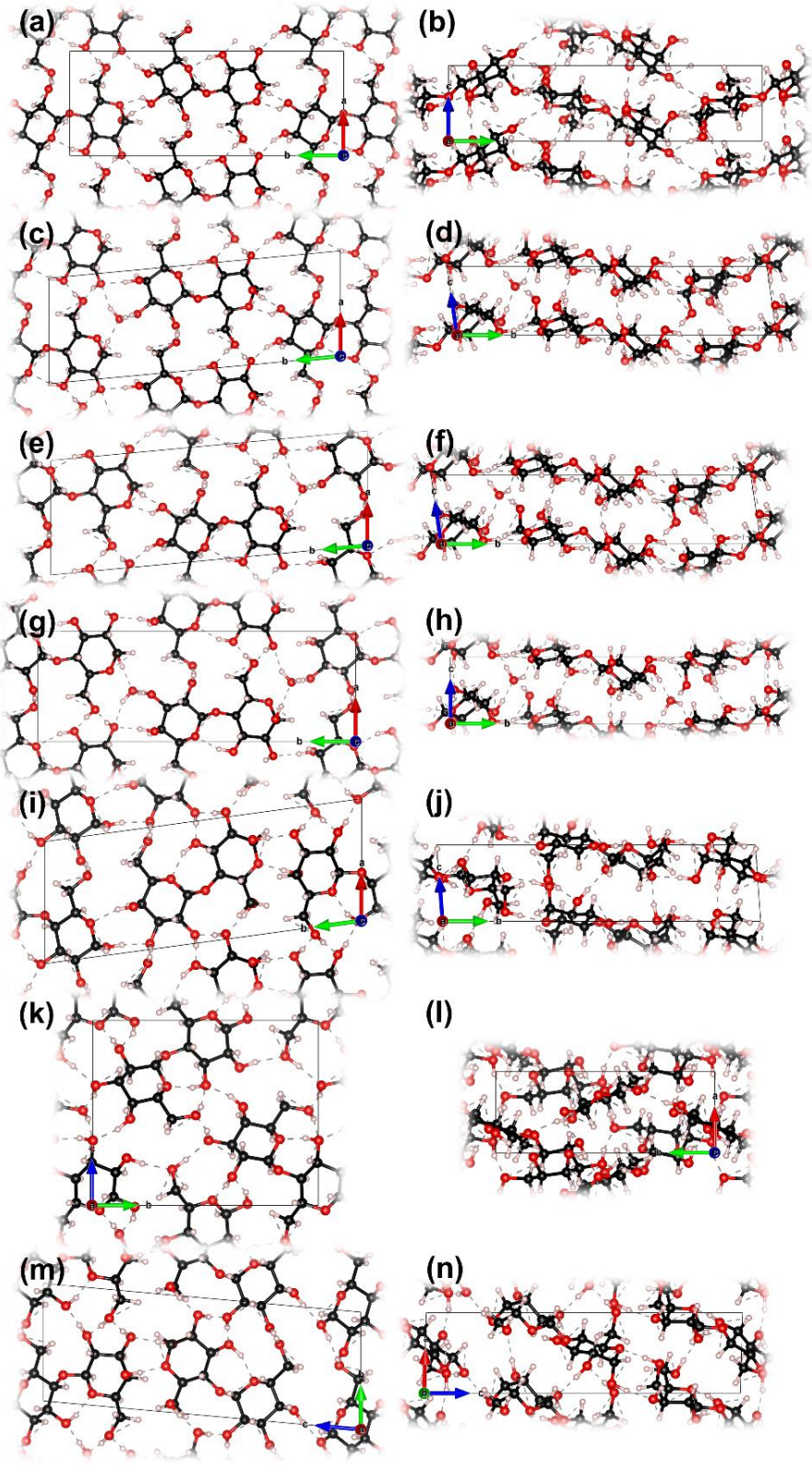

Fig. S4: Ball-and-stick representation of the different molecular crystal structures studied in this work. For each of the systems, we present a "top" view (a: α-LH, c: α-LHa, e: α-LHb, g: α-LM, i: α-LA, k: β-L, m: αβ-L) and a "side" view (b: α-LH, d: α-LHa, f: α-LHb, h: α-LM, j: α-LA, l: β-L, n: αβ-L). A single unit-cell is indicated by the black quadrilateral. Lattice-vectors are indicated by the coloured arrows, and potential hydrogen bridges – suggested by the VESTA plotting software[1] – are indicated as grey dashed lines. The molecular lattice is extended beyond the bounds of a single unit cell to provide a clearer picture of the molecular bonding.

[1] K. Momma and F. Izumi, "VESTA 3 for three-dimensional visualization of crystal, volumetric and morphology data," J. Appl. Crystallogr., 44, 1272-1276 (2011).

5.4. PES of water rotation in α-Lactose Monohydrate

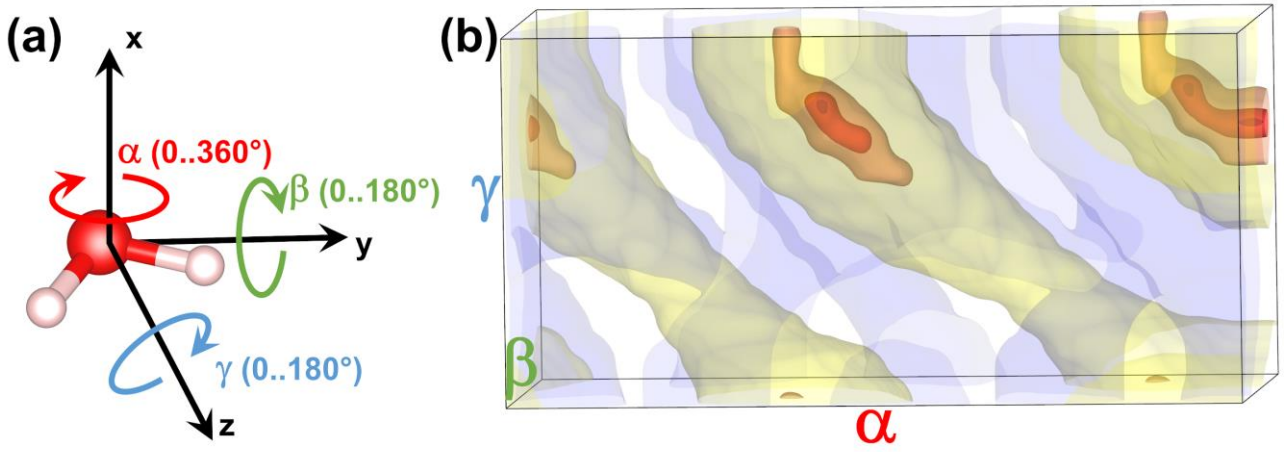

Fig. S5: (a) The three Tait-Bryan rotation angles of a water molecule. (b) The PES of a single water rotation in α-Lactose Monohydrate (single-point energies). Isosurfaces are indicated, with red lowest energy, and blue for higher energies.

Table S4: The low THz modes of the configurations containing a rotated water molecule. A visual representation of the spectra is shown in Fig. 9b. Values between brackets are those of the configuration without structure optimization. No corrections are performed for Pulay stresses. The reference system with the water molecules fully optimized is indicated as A. Frequencies are given in THz.

mode	A	B	B′	C
1	0.589	0.551 (0.565)	0.616 (0.590)	0.579 (0.568)
2	1.079	1.088 (1.075)	1.066 (1.070)	1.041 (1.028)
3	1.173	1.135 (1.170)	1.192 (1.152)	1.150 (1.204)
4	1.347	1.343 (1.315)	1.361 (1.339)	1.239 (1.428)
5	1.502	1.506 (1.512)	1.482 (1.489)	1.616 (1.532)

5.5. Gas-phase clusters of a single molecule α-Lactose and water

Table S5: Donor or acceptor role of water of the hydrogen bond formed towards α-lactose.

	Single α-lactose molecule	Position A: water as H-bond donor	Position A': water as H-bond acceptor	Position B: water as H-bond acceptor	Position B': water as H-bond donor
System	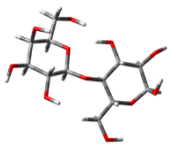	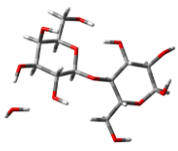	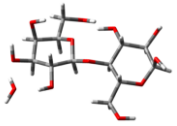	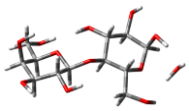	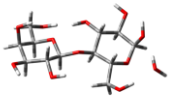
ΔE, kcal/mol	–	0.00	-5.51	-3.13	-2.78
Frequency, cm^{-1} (THz)	0.70 (23.26)	0.62 (20.54)	0.58 (19.34)	0.586 (19.54)	0.63 (20.97)
	1.08 (36.08)	1.03 (34.44)	0.99 (32.98)	0.945 (31.51)	0.89 (29.56)
	1.26 (42.06)	1.12 (37.35)	1.14 (37.99)	1.178 (39.28)	1.21 (40.35)
	1.83 (61.13)	1.21 (40.60)	1.23 (41.07)	1.555 (51.88)	1.33 (44.36)
	2.22 (74.18)	1.82 (60.72)	1.80 (59.97)	2.116 (70.58)	1.74 (58.18)
	2.72 (90.78)	2.23 (74.36)	2.21 (73.61)	2.515 (83.90)	2.18 (72.83)
	2.94 (97.98)	2.68 (89.25)	2.96 (98.80)	2.912 (97.15)	2.48 (82.65)
	3.17 (105.85)			2.924 (97.55)	3.13 (104.65)
					3.19 (106.41)

5.6. Calculated IR-intensities of the lowest THz modes

The IR-intensities of the different lactose configurations were calculated based on the Born Effective Charge scheme[2,3] and are presented in the Table S6. The IR intensities are extremely small due to the delocalized nature of the THz vibrations (*i.e.*, the vibration is smeared out over a large number of atoms) in contrast to the high frequency modes generally investigated using IR-spectroscopy which tend to be localized on only a few bonds. Without performing a full study, the following are illustrative examples hereof:

a) Entire system is oscillating, e. g.
   0.588 THz → I = 0.0008506
   1.5016 THz → I = 0.0038385

b) Localized vibrations, e. g.

   4.755 THz: O of water wobbles → I = 0.0143585
   16.147 THz: water rotates → I = 0.1071180

The animation of the modes at ~ 0.6 THz, ~1.5 THz and ~ 4.8 THz (includes as separate .gif files), also readily show that in the system under study, already above 4THz (which is far beyond the upper-bound of the range we present) the modes are much more localized.

As such, the IR-intensities are presented for comparative purposes with the other calculations. All intensities are provided as fraction of the maximum peak intensity (bottom line of the Table).

Table S6: Calculated IR intensities.

α-LM		α-LHb		α-LHa		α-LH		α-LA		αβ-L		β-L	
THz	I (%)	THz	I (%)	THz	I (%)	THz	I (%)	THz	I (%)	THz	I (%)	THz	I (%)
2.62	0.0056	**2.61**	0.1580	**2.62**	0.1178	**2.90**	0.1056	**2.78**	0.0297	**2.69**	0.0380	**2.61**	0.0252
2.39	0.0095	**2.53**	0.0239	**2.41**	0.0365	**2.69**	0.0666	**2.60**	0.0797	**2.42**	0.1003	**2.57**	0.0557
1.97	0.0304	**2.20**	0.0289	**2.21**	0.0105	**2.47**	0.0450	**2.50**	0.0405	**2.21**	0.0216	**2.48**	0.0149
1.84	0.0012	**1.91**	0.0973	**1.98**	0.0602	**1.68**	0.0298	**2.10**	0.2674	**2.11**	0.0671	**2.31**	0.3692
1.47	0.0693	**1.60**	0.0741	**1.53**	0.0719	**1.55**	0.0893	**1.81**	0.0296	**1.84**	0.0062	**2.12**	0.0754
1.30	0.0043	**1.30**	0.0191	**1.31**	0.0144	**1.54**	0.0523	**1.67**	0.0684	**1.70**	0.0207	**1.86**	0.0002
1.09	0.0012	**1.21**	0.0357	**1.23**	0.0377	**1.38**	0.0366	**1.22**	0.0106	**1.21**	0.0104	**1.74**	0.1705
1.04	0.0004	**1.05**	0.0073	**0.99**	0.0036	**1.20**	0.0166	**0.98**	0.0441	**0.85**	0.0147	**1.64**	0.0112
0.55	0.0154	**0.74**	0.1045	**0.74**	0.1082	**1.03**	0.0636	**0.89**	0.0008	**0.82**	0.0158	**1.39**	0.0622
Highest IR-intensity peak, absolute value intensity													
THz	I	THz	I	THz	I	THz	I	THz	I	THz	I	THz	I
97.28	5.5414	**100.43**	2.6850	**92.82**	2.4948	**94.38**	4.0585	**98.95**	3.0589	**98.54**	3.7218	**96.30**	4.1570

5.7. SEM images

The surface of the lactose pellet was investigated by means of scanning electron microscopy (Supra55VP) before heating and shortly after each set of the heating manipulations (to 104°C and 150°C). The SEM images taken around the pellet centre for the three cases are presented in Fig. S6.

[2] https://journals.aps.org/rmp/abstract/10.1103/RevModPhys.73.515

[3] https://github.com/dakarhanek/VASP-infrared-intensities

After the heating of the pellet to 104°C and the following cooling, the pellet surface turned to be covered by "fissures" – quite normal for the dry matter (Fig. S6b). With stronger magnification (x10), it is still difficult to see a considerable difference of the surface structure (compare Fig. S6a' and Fig. S6b').

Contrary, after the heating up to 150°C the pellet surface is covered with chaotically oriented, prolonged (~ 1000nm*100nm) structures – another indication for the change in the lactose crystal phase.

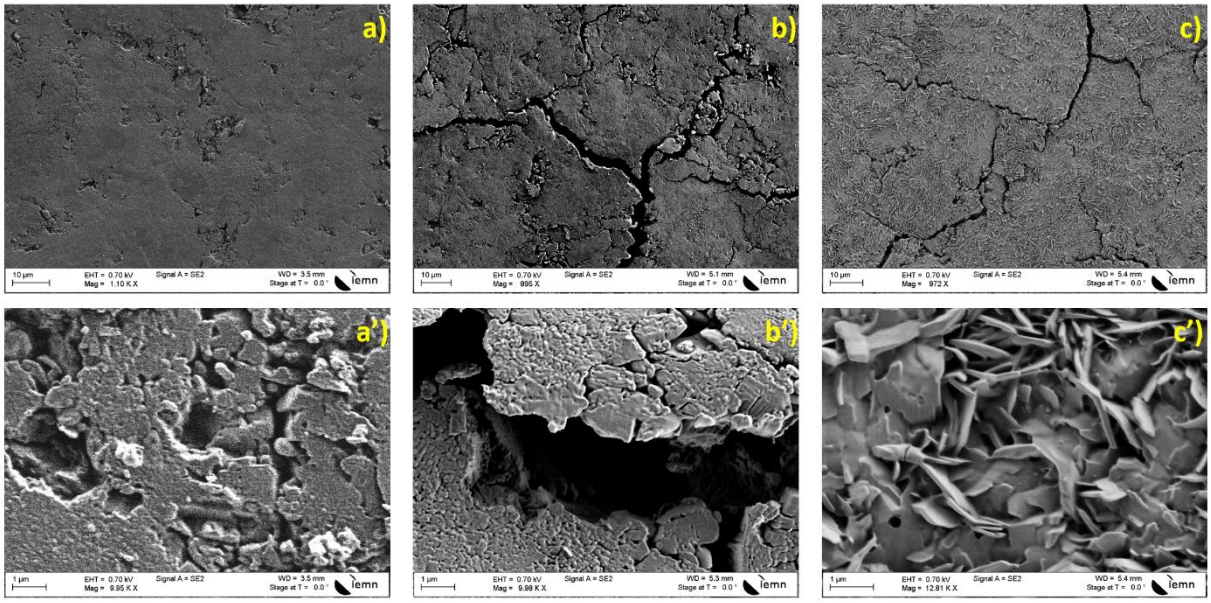

Fig. S6: SEM images of the pellet centre for the three phases 1(a) – 3(c). Top row – larger scale. Bottom row – zoomed.